

## PHOTOTHERMAL LENGTH MEASUREMENT OF VICKERS CRACKS IN $\text{Si}_3\text{N}_4$

Jukka Rantala, Jari Hartikainen, Reijo Lehtiniemi, Reijo Vuohelainen, and Mauri Luukkala

University of Helsinki  
Department of Physics  
Siltavuorenpenger 20 D  
SF-00170 HELSINKI  
Finland

Jussi Jaarinen

Neste OY, Corporate R&D  
P. O. BOX 310  
SF-06101 Porvoo, Finland

### INTRODUCTION

Ceramic materials are gaining ever increasing popularity in different high-technology applications, especially in those where high temperatures are used. However, the mechanical strength of ceramics has thus far set limitations on their utilizing. The critical size of cracks in ceramic material depends on the force applied, but in typical applications it is less than 100  $\mu\text{m}$ . This small size in addition to the fact that critical cracks are often closed makes the use of conventional NDT methods in crack detection very difficult or even impossible. More nuisance comes from the porosity of the material which takes methods needing immersing in liquids out of consideration.

Together with the detection and measuring of critical cracks there is also another motivation for exact crack length measurement. Fracture toughness of material can be determined by making an artificial indentation on the sample surface and measuring the lengths of generated cracks. So far the results of this kind of fracture toughness measurements have not been very encouraging which could be due to optical measurements used that might give results shorter than the real lengths.

This study is divided into three parts. First we describe theoretical calculations of temperature distribution near the end of a closed vertical crack. Then we present the results of artificial Vickers crack length

measurements made by photothermal microscope. These results are compared with the values obtained using optical microscope. The samples used were both hot-pressed and sintered  $\text{Si}_3\text{N}_4$  with the commercial names Shiganawa and Ekasin. The load used in the indentations was 10 kg.

In the third part of this paper we present study of some real, not artificial, cracks. Defective zirconia samples were measured photothermally to find the phase lag caused by a crack. After these thermal measurements the samples were broken using four point bending to determine the bending strength.

## THEORY

In many applications of thermal microscopy a sample is heated periodically producing a wave-like temperature distribution (Fig 1). The resulting temperature distribution in the sample can be described using the heat diffusion equation

$$\nabla \cdot (K \nabla T) + G = \rho c \frac{\partial T}{\partial t} \quad (1)$$

where  $T$  is the temperature,  $K$  is the thermal conductivity,  $\rho$  is the density, and  $c$  is the specific heat of the sample.  $G$  is the heating power per unit volume.

Sinusoidal periodical heating with angular frequency  $\omega$  results in the temperature

$$T(\vec{r}, t) = \tau(\vec{r}) \exp(i\omega t) \quad (2)$$

Assuming that no heat is generated in the sample and the heat conductivity is uniform and doesn't depend on the temperature, the spatial part of eq. (1) can be written

$$\frac{K \nabla^2 \tau}{\rho c i \omega} = \tau \quad (3)$$

The boundary conditions of the diffusion equation are obtained from the continuity of temperature and heat flow at all interfaces. On the upper surface,  $z=0$ , of the sample this is obtained through the heating beam intensity. Cracks hindering the heat conduction can be described as internal interfaces in the sample having a specified thermal contact resistance.

When the depth of the crack is finite and the length semi-infinite the boundary conditions make the diffusion equation (3) too complicated to be solved analytically. We solved this equation using finite difference method and Gauss-Seidel iteration.

In our model the sample consisted of three-dimensional grid where the crack was as an internal interface in the middle of two neighboring grid points (Fig. 2). The thermal contact resistance caused by the crack determines its severeness. The total thermal resistance between the points (i-1, j, k) and (i, j, k) is the sum of thermal resistances in faultless material,  $\Delta x/2K$ , and the thermal contact resistance caused by the crack,  $R_c$

$$R = \frac{\Delta x}{2K} + R_c + \frac{\Delta x}{2K} = \frac{\Delta x}{K} + R_c \quad (4)$$

This way we can define effective thermal conductivity  $K_{eff}$

$$K_{eff} = \frac{\Delta x}{R} = \frac{K \Delta x}{\Delta x + K R_c} \quad (5)$$

to get the solution algorithm simpler. Now the only thermal parameter that is not uniform in the sample is effective thermal conductivity which is used in the calculations instead of  $K$ .

In the calculations line scans over the crack were simulated. The positions of these scan lines in respect to the crack are marked with Y-coordinates in Fig. 3a. The distance perpendicular to the crack is marked using X-coordinates. In Fig. 3b the crack profile used in these calculations is shown. A typical industrial  $\text{Si}_3\text{N}_4$  was selected as a model material and thus the following values of the thermal properties were chosen: 25 W/(K m) for thermal conductivity, 800 J/(kg K) for specific heat, and 3200 kg/m<sup>3</sup> for density. The characters of the thermal microscope were also typical for photothermal microscopy purposes being 10 mW for the heating power and 5.0  $\mu\text{m}$  for the 1/e-radius of the heating beam.

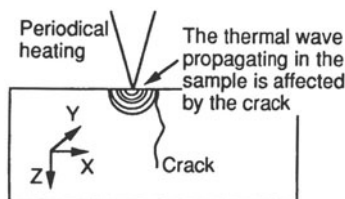


Fig. 1. Thermal wave production in the sample.

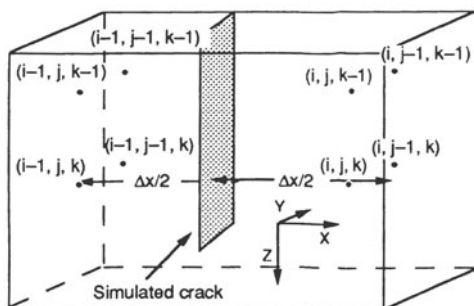


Fig. 2. The placement of the crack in the 3-dimensional grid.

As an example magnitude and phase figures of a special case where no heat flow through the crack occurs (thermal contact resistance  $1 \cdot 10^{10} \text{ m}^2\text{K/W}$ ) are presented in Fig. 4. It can be seen that the effect of the crack ends very quickly when the crack ends and at the distances of 10 to 15  $\mu\text{m}$  it can no more be detected in measurements. Calculations made with other modulation frequencies (1.0 – 16.0 kHz) and values of thermal contact resistances ( $1 \cdot 10^{-8} - 1 \cdot 10^{-5} \text{ m}^2\text{K/W}$ ) gave similar kind of results and showed that the determination of the vertical crack length is not sensitive to the modulation frequency, which is consistent with earlier studies of resolution made with other kind of defects [1,2,3,4,5,6,7].

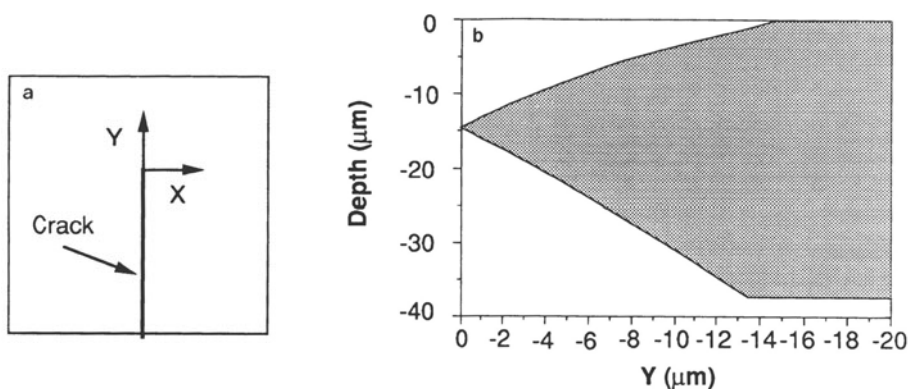


Fig. 3. a) The coordinates and b) the crack profile used in presentation of theoretical temperature curves.

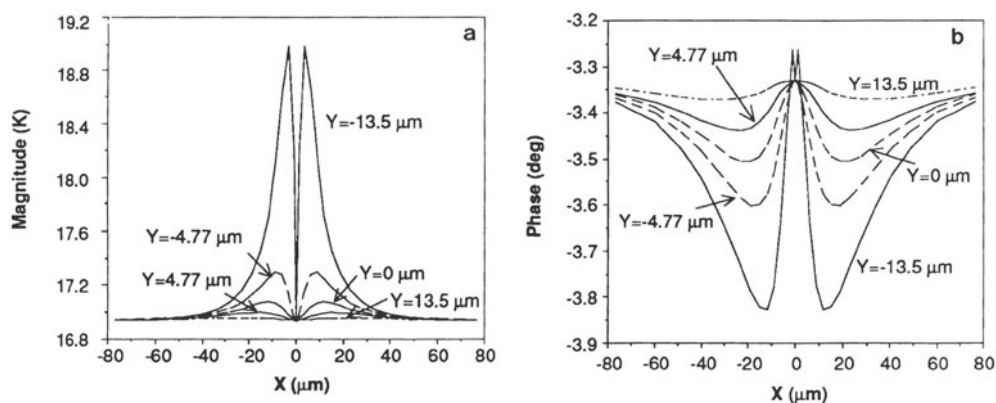


Fig. 4. Magnitude and phase figures representing line scans made from various distances from the end of the crack. Value of the modulation frequency used was 1.0 kHz and no heat flow through the crack.

## MEASUREMENT SYSTEM

For crack detection we used the optical beam deflection (OBD) method which is also called mirage method. This was first introduced by Boccara et al. [8]. This detection method is especially suitable for vertical crack detection because of its sensitivity for transversal heat flux [9].

The sample was heated with an  $\text{Ar}^+$  laser with powers of 15 to 40 mW. After the amplitude modulation made by acousto-optic modulator the beam was focused on the sample surface with a microscope lens giving the value of  $5.0\text{ }\mu\text{m}$  for the  $1/e$  -radius of the focus. The radius was measured using a razor edge. The probe beam was a HeNe laser that was focused using a lens of 120 mm focal length. The probe beam deflection was detected using a quad type position sensitive detector whose signal was input of a lock-in amplifier. The data was collected with a micro computer that also controlled the xy translation stage that moved the sample under the heating beam. In the crack length measurements several different horizontal and vertical offset values of the probe beam were used. To study the effect of the modulation frequency to the measured length of the crack frequencies of 1.0, 2.0, 4.0, 8.0, and 16.0 kHz were used. Zirconia samples were measured using modulation frequency of 1.0 kHz.

## EXPERIMENTAL RESULTS

### Vickers crack measurements

A typical thermal image of a Vickers indentation and cracks in  $\text{Si}_3\text{N}_4$  is shown in Fig. 6.

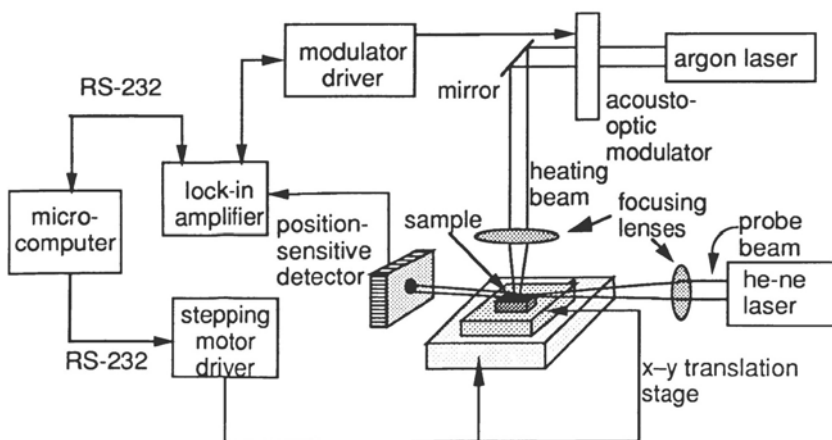


Fig. 5. A schematic view of the photothermal microscope used for crack detection.

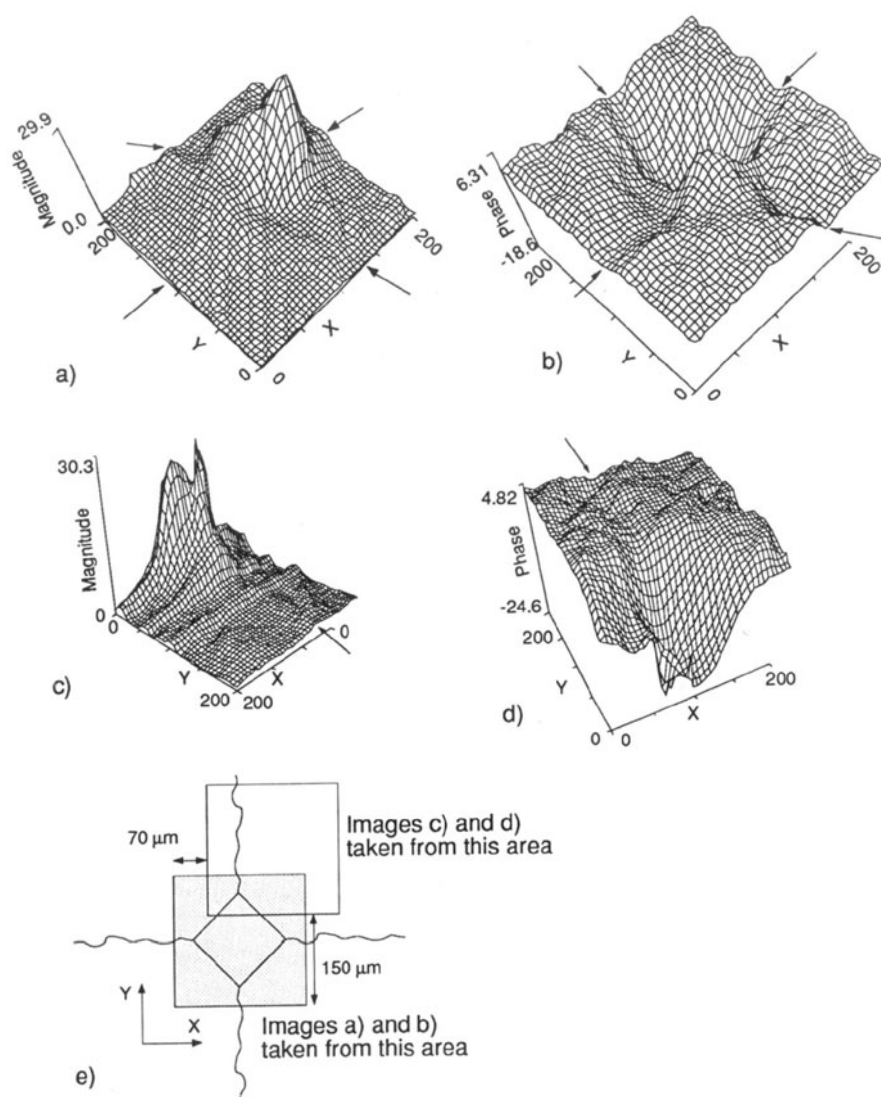


Fig. 6. Thermal magnitude (a, c) and phase (b,d) images of a Vickers indentation and cracks (marked with arrows) originating from it. Location of the images in respect to the indentation is shown in figure e). Both magnitude and phase values are scaled to the mean value. The x and y coordinates are in micro-meters. Sample was sintered Shiganawa. The figures presented here are taken using transversal signal and modulation frequency of 1.0 kHz.

Table 1. Comparison of optically and thermally measured cracks. Distances are in micrometers and the measurement raster density parallel to the crack are in parentheses.

sintered Shiganawa		hot-pressed Ekasin	
thermal	optical	thermal	optical
515 (+22)	251	420 (+15)	227
370 (+20)	235	370 (+20)	276

In Table 1 the lengths of the Vickers cracks measured using thermal and optical microscopes are listed.

The thermally detected lengths were measured as the distance between the outer raster points where the crack can still be seen. The measured crack length doesn't depend on the modulation frequency used which agrees with the theoretical calculations described earlier in this paper.

Measurements of real cracks in zirconia samples

After the photothermal detection of cracks zirconia samples were broken using four-point bending. The phase lag caused by the crack situated at the breaking location is shown in Fig. 7 as a function of the bending force needed to break the sample. As expected, the obtained phase lag gets smaller when the force, and thus the bending strength, becomes bigger. The correlation is not very good which can be explained by the fact that all the samples were not similar. In addition to the cracks there were differences in porosity and other volume defects which also affects the bending strength.

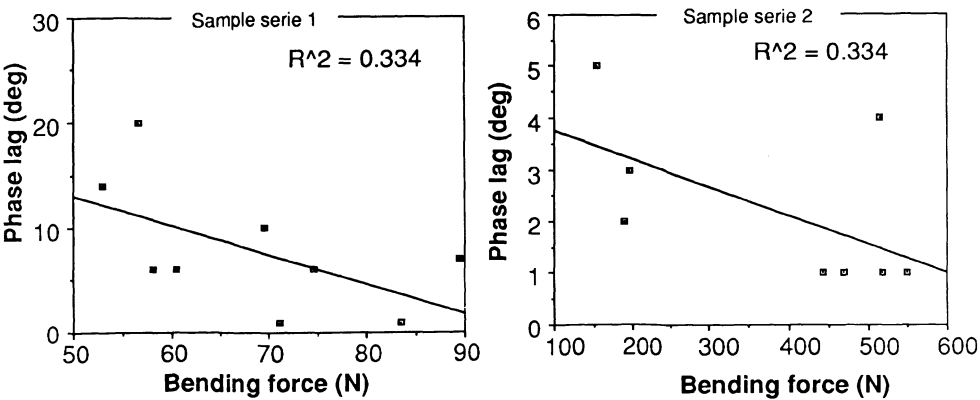


Fig 7. The phase lag as a function of bending force and the line fitted to the measurement points. Correlation coefficient squared is shown in upper right hand corner.

## CONCLUSIONS

In all cases the thermally measured Vickers crack lengths were more than 90 micrometers longer than the optically measured ones. As the numerical calculations show, the effect of the crack on the thermal measurement ends in the distance of 10 – 15  $\mu\text{m}$  from the end of the crack. Because of this it can be assumed the longer lengths obtained thermally cannot be due to thermal diffusion. Either the cracks extend under the surface or they are simply so small that they cannot be seen. Modulation frequency and does not affect the thermally measured crack length in practical sense. Volume defects give nuisance for bending force determination using photothermal microscopy.

## ACKNOWLEDGEMENTS

The authors would like to thank E. Levänen and A.-P. Nikkilä at Tampere University of Technology, who provided us with the Vickers indented samples and optically measured the lengths of the cracks, and WP Ceramics Ltd which gave us the zirconia samples and made the bending strength measurements.

## REFERENCES

1. L. J. Inglehart: Optical Beam Deflection Detection of Thermal Waves in Opaque Solids, Dissertation, Wayne State University, Detroit, Mich. (1984)
2. L. J. Inglehart, K. R. Grice, L. D. Favro, P. K. Kuo, R. L. Thomas: Appl. Phys. Lett. 43, 446 (1983)
3. L. J. Inglehart, M. J. Lin, L. D. Favro, P. K. Kuo, R. L. Thomas: In Proc. IEEE Ultrason. Symp., ed. by B. R. McAvey (Institute of Electrical and Electronic Engineers, New York 1983) p. 668
4. F. A. McDonald, C. G. Wetsel: In Proc. IEEE Ultrason. Symp., ed. by B. R. McAvey (Institute of Electrical and Electronic Engineers, New York 1984) p. 622
5. L. D. Favro, P. K. Kuo, R. L. Thomas: In Photoacoustic and Thermal Wave Phenomena in Semiconductors, ed. by A. Mandelis (North Holland Publishing, Amsterdam 1987) p.68
6. F. A. McDonald, C. G. Wetsel, C. G. Clark: In Proc. IEEE Ultrason. Symp., ed. by B. R. McAvey (Institute of Electrical and Electronic Engineers, New York 1983) p.672
7. P. K. Kuo, L. D. Favro, L. J. Inglehart, R. L. Thomas, M. Srinivasan: J. Appl. Phys. 53, 1258 (1982)
8. A. C. Boccara, D. Fournier, J. Badoz: Appl. Phys. Lett. 36, 130 (1980)
9. K. R. Grice, L. J. Inglehart, K. D. Favro, P. K. Kuo, R. L. Thomas: J. Appl. Phys. 54, 6245 (1983)